Rad52 forms DNA repair and recombination centers during S phase

Michael Lisby*, Rodney Rothstein*†, and Uffe H. Mortensen‡

*Department of Genetics and Development, Columbia University, College of Physicians and Surgeons, 701 West 168th Street, New York, NY 10032-2704; and ‡Center for Process Biotechnology, BioCentrum-DTU, Technical University of Denmark, Building 223, DK-2800 Lyngby, Denmark

Maintenance of genomic integrity and stable transmission of genetic information depend on a number of DNA repair processes. Failure to faithfully perform these processes can result in genetic alterations and subsequent development of cancer and other genetic diseases. In the eukaryote *Saccharomyces cerevisiae*, homologous recombination is the major pathway for repairing DNA double-strand breaks. The key role played by Rad52 in this pathway has been attributed to its ability to seek out and mediate annealing of homologous DNA strands. In this study, we find that *S. cerevisiae* Rad52 fused to green fluorescent protein (GFP) is fully functional in DNA repair and recombination. After induction of DNA double-strand breaks by γ-irradiation, meiosis, or the *HO* endonuclease, Rad52-GFP relocalizes from a diffuse nuclear distribution to distinct foci. Interestingly, Rad52 foci are formed almost exclusively during the S phase of mitotic cells, consistent with coordination between recombinational repair and DNA replication. This notion is further strengthened by the dramatic increase in the frequency of Rad52 focus formation observed in a *pol12-100* replication mutant and a *mec1* DNA damage checkpoint mutant. Furthermore, our data indicate that each Rad52 focus represents a center of recombinational repair capable of processing multiple DNA lesions.

Homologous recombination is responsible for a number of important DNA processes, including efficient and precise repair of DNA double-strand breaks (DSBs), maintenance of telomere length and rDNA copy number, and generation of genetic diversity during meiotic recombination (1–3). Genetic, physical, and biochemical analyses of various recombination reactions have identified a number of key DNA intermediates in this process. These include a DNA DSB, 3′ single-stranded tails and double Holliday junctions. At the level of DNA, these intermediates have been incorporated into the double-strand break repair model for homologous recombination (4, 5). *RAD52* is essential for efficient homologous recombination in *Saccharomyces cerevisiae* (1, 6, 7) and is the genetic marker most frequently used to define this process. The importance of Rad52 is underscored by the fact that its primary structure and biochemical properties are conserved from yeast to humans (8–11). However, disruption of the *RAD52* gene in chicken and mouse causes only a minor reduction in homologous integration frequencies and has little or no effect on repair of DNA damage induced by ionizing radiation (12, 13). Therefore, in higher eukaryotes it is possible that the absence of Rad52 can be relieved by an alternative repair pathway or by a redundant Rad52. The latter view is supported by the finding that the fission yeast, *Schizosaccharomyces pombe*, contains two *RAD52* homologues (14, 15).

Biochemically, Rad52 has been shown to bind single- and double-stranded DNA with a preference for DNA ends (16–18). In addition, Rad52 provides a physical link between the single-strand DNA binding replication protein complex, RP-A, and the RecA homologue, Rad51 (10, 19–21). The collaboration of these three factors accomplishes efficient strand exchange reactions *in vitro* (22–24). Perhaps the ability of Rad52 to provide a bridge between the DNA replication machinery and the Rad51 recombinase explains the severe biological defects that are observed in its absence. In addition, Rad52 forms heptameric ring structures that accumulate on single-stranded DNA molecules *in vitro* (25, 26). Because similar aggregates of Rad52 could assemble locally on DNA during homologous recombination and potentially be visualized by microscopy *in vivo*, we tagged Rad52 with green fluorescent protein (GFP). The resulting Rad52-GFP fusion protein is biologically competent and, consequently, it constitutes an excellent molecular marker to evaluate homologous recombination and DNA DSB repair *in vivo*. Here we use Rad52-GFP to demonstrate that formation of Rad52 foci is a universal trait of Rad52-dependent recombination and DNA repair processes. Importantly, we find that each Rad52 aggregate is capable of processing multiple DNA lesions. Furthermore, these putative DNA repair and recombination centers are coupled to S phase, thus providing a strong link between homologous recombination and DNA replication.

Materials and Methods

Yeast Strains and Media. Yeast strains used in these studies are shown in Table 1. Yeast extract-peptone-dextrose (YPD) medium, synthetic complete (SC) medium, synthetic complete without leucine (SC-Leu), and 5′-fluoroorotic acid (5-FOA) were prepared as described (27). Yeast extract-peptone-acetate (YEPA): 10 g/l yeast extract, 20 g/l peptone, and 20 g/l potassium acetate. Sporulation (SPO) medium: 2.5 g/l yeast extract and 15 g/l potassium acetate supplemented with 62 mg/l leucine and 20.6 mg/l of adenine, histidine, tryptophan, and uracil, respectively.

Construction of the *RAD52-GFP* Fusion Gene. A red-shifted enhanced version (10C) of the GFP gene (28) was a generous gift from R. Tsien (University of California, San Diego, La Jolla, CA). This version of GFP was fused by PCR to either the 5′- or 3′-two-thirds of the *Kluyveromyces lactis URA3* gene, using adaptamer technology (29, 30). Next, the resulting fragments were ligated into the *Sac*II site of pRS423 (31) to produce plasmids pWJ1164 and pWJ1165. By using the principle in our previously described allele replacement method (32), these plasmids serve as basic tools to target GFP specifically to any site in the genome. In brief, two GFP-*URA3* PCR products were amplified from pWJ1164

This paper results from the National Academy of Sciences colloquium, ''Links Between Recombination and Replication: Vital Roles of Recombination,'' held November 10–12, 2000, in Irvine, CA.

Abbreviations: DAPI, 4′,6-diamidino-2-phenylindole; GFP, green fluorescent protein; DSB, double-strand break; YPD, yeast extract-peptone-dextrose; SC, synthetic complete; SPO, sporulation.

†To whom reprint requests should be addressed. E-mail: rothstein@cancercenter.columbia.edu.

www.pnas.org/cgi/doi/10.1073/pnas.121006298

Table 1. Yeast strains used in this study

Strain*	Genotype
W2681	*MAT***a**/*MATα lys2Δ/LYS2 TRP1/trp1-1 leu2-ΔEcoRI/leu2-ΔBstEII*
W2682	*MAT***a**/*MATα lys2Δ/LYS2 TRP1/trp1-1 leu2-ΔEcoRI/leu2-ΔBstEII RAD52-GFP/RAD52-GFP*
W2683	*MAT***a**/*MATα lys2Δ/LYS2 TRP1/trp1-1 leu2-ΔEcoRI/leu2-ΔBstEII RAD52-GFP/RAD52-GFP spo11Δ/spo11Δ*
W2297-12D	*MAT***a** *LYS2 trp1-1 bar1::LEU2 leu2-3,112*
W2297-4A	*MAT***a** *LYS2 trp1-1 bar1::LEU2 leu2-3,112 RAD52-GFP*
W2381-10B	*MAT***a** *LYS2 trp1-1 bar1::LEU2 leu2-3,112 RAD52-GFP mec1Δ::TRP1 sml1Δ::HIS3*
W2382-2A	*MAT***a** *LYS2 trp1-1 bar1::LEU2 leu2-3,112 RAD52-GFP sml1Δ::HIS3*
J861	*MAT***a** *LYS2 trp1-1 bar1::LEU2 leu2-3,112 RAD52-GFP rho^0*
W2366-6B	*MAT***a** *LYS2 trp1-1 bar1::LEU2 leu2-3,112 rad52Δ::HIS5*
W2796	*MAT***a**/*MATα lys2Δ/LYS2 leu2-ΔEcoRI/leu2-ΔBstEII rad52Δ::HIS5/rad52Δ::HIS5 TRP1/trp1-1*
UM10-25D	*MAT***a** *LYS2 trp1-1 bar1::LEU2 leu2-3,112 RAD52-GFP pol12-100*
W2334-1D	*MAT::HIS3 LYS2 trp1-1 leu2-3,112 RAD52-GFP*
W2613-22A	*MAT::HIS3 LYS2 trp1-1 RAD52-GFP leu2-ΔEcoRI::URA3-HO::leu2-ΔBstEII*
W2322-8A	*MAT***a** *LYS2 trp1-1 RAD52-GFP leu2-ΔEcoRI::URA3-HO::leu2-ΔBstEII*
W2322-5B	*MAT***a** *LYS2 trp1-1 leu2-3,112 RAD52-GFP*

*All strains in this study are derivatives of W303-1A and W303-1B (67). In addition to the genotype listed above, all strains are *RAD5 can1-100 ura3-1 his3-11,15 ADE2*.

and pWJ1165 by using appropriate primers (GFPstart-F: 5′-ATGAGTAAAGGAGAAGAAC-3′, URA3int-R: 5′-GAGCAATGAACCCAATAACGAAATC-3′ and GFPend-R: 5′-TTTGTATAGTTCATCCATGC-3′, URA3int-F: 5′-CTTGACGTTCGTTCGACTGATGAGC-3′, respectively; Fig. 1*A*). Next, two pairs of PCR primers were designed to amplify ≈400 base pairs *u*pstream (UF: 5′-CCTTTGTTACAGCTAAGGC-3′, URtag1: 5′-gttcttctcctttactcatCCCAGTAGGCTTGCGTGCATG-3′) and *d*ownstream (DFtag2: 5′-ggatgaactatacaaataaCCCGCTTCCTGGCCGAAAC-3′, DR: 5′-AATGAACCTAAGGATTCCGC-3′) of the GFP insertion site at the 3′ end of *RAD52* by using genomic DNA (or plasmid DNA) as a template (Fig. 1*A*). The upstream and downstream fragments each contain an additional 19 base pairs of DNA sequence (tag1 and tag2 shown in small letters) complementary to parts of the two GFP-*URA3* PCR products amplified from pWJ1164 and pWJ1165. The reverse and complementing sequences at the ends (the tags) facilitate the fusion of the two pairs of PCR products to generate the two fragments shown in Fig. 1*B*. After cotransformation of these two PCR products into W2109-14C, *in vivo* homologous recombination generates a GFP direct repeat flanking an intact *K. lactis URA3* gene downstream of *RAD52* (Fig. 1*C*). Loss of the *URA3* gene resulting from direct repeat recombination is selected on 5-FOA medium to generate a "clean" genomic *RAD52-GFP* fusion. Western blot analysis of Rad52 was performed essentially as described (16) except that the Rad52 antibody was affinity purified according to standard procedures by employing a Rad52-Sepharose 4B resin.

Microscopy. Unless otherwise noted, all experiments were performed at 23°C to allow the GFP chromophore to form efficiently (32). Before epifluorescence microscopy, cells were washed twice in either SC (mitotic experiments) or SPO (meiotic experiments) medium. Next, cells were immobilized on a glass slide by mixing them with a 37°C solution of 1.2% (wt/vol) low melting agarose (NuSieve 3:1 from FMC) containing the appropriate medium. To prevent evaporation, the cover glass was sealed with a mixture of equal volumes of molten bees' wax, petroleum jelly (VWR Scientific), and lanolin (Sigma). The filters used to visualize Rad52-GFP (excitation 480 nm; emission 535 nm) and 4′,6-diamidino-2-phenylindole (DAPI; excitation 365 nm, emission 450 nm) were from Omega Optical (Brattleboro, VT). Images were acquired by using a cooled CCD camera (Star-1 from Photometrics, Tucson, AZ) mounted on a Zeiss Axioplan II microscope with a Plan-Apochromat 100×, 1.4 numerical aperture (NA) objective lens. The illumination source was a 100-W mercury arc lamp. Images were obtained at 0.2-μm intervals along the *z* axis by using a piezo-controlled stepper and Rad52-GFP foci were counted by inspecting all of the focal planes intersecting each cell. Integration time for acquisition of the fluorescent images was 200 ms. Images were acquired in the IP LAB software (Scanalytics, Billerica, MA) and prepared for publication in SCION V1.62 (National Institutes of Health) and ADOBE PHOTOSHOP (Adobe Systems, Mountain View, CA).

DNA in living cells was stained for visualization by adding 10 μg/ml DAPI to the culture 30 min before imaging. Selected strains were made rho^0 (mitochondrial DNA negative) before staining to eliminate any signal from mitochondrial DNA (27). Localization of Rad52-GFP was not affected by the absence of mitochondria nor by DAPI staining (data not shown).

γ-Irradiation. The γ-ray sensitivities of strains were determined by growing cultures in YPD to mid-log phase at 23°C. An appropriate number of cells were plated on YPD plates and exposed to different doses of γ-rays by using a Gammacell-220 ^{60}Co irradiator (Atomic Energy, Ottawa). Cells analyzed by microscopy were pregrown in YPD at 23°C until OD_{600} reached 0.2. At this point, the liquid cultures were exposed to defined doses of irradiation and aliquots of the cultures were processed immediately for imaging.

To estimate the number of *rad52*-repairable lesions induced by γ-irradiation, we made the following two assumptions: (*i*) γ-ray-induced DNA damage occurs randomly in a population of cells and (*ii*) one *rad52*-repairable lesion is sufficient to kill a cell (33). The number (n) of γ-ray-induced DNA lesions per cell that are lethal in the absence of *RAD52* can be described by a Poisson distribution [$P_n(x) = e^{-\mu}\mu^n/n!$, $-\mu = kx$, $n = 0, 1, 2, \ldots$, where x is the γ-ray dose and μ the mean number of lethal lesions per cell at that dose]. Accordingly, the probability of a cell surviving a given γ-ray dose (x) is $P_0(x) = e^{kx}\mu^0/0! = e^{kx} \Rightarrow \ln(P_0(x)) = kx$. By fitting the γ-ray survival curve of *rad52*Δ strains (Fig. 2*B*) to this equation, k is estimated to be -0.5. Thus, the γ-ray dose required to generate an average of one *rad52*-repairable lesion per cell ($\mu = 1$) is $-\mu/k = -1/-0.5 = 2$ krad.

Induction of DSBs by the *HO* Endonuclease. Strains containing no, one, or two accessible *HO*-cut sites were transformed with pJH132 (kindly provided by Jim Haber, Brandeis University, Waltham, MA) containing a galactose-inducible *HO* gene and a *TRP1* selectable marker (34). Transformants were grown at 23°C in SC-Trp (W2334–1D and W2322–5B) or SC-Trp-Ura (W2613–22A and W2322–8A) medium containing 2% raffinose. At

COLLOQUIUM

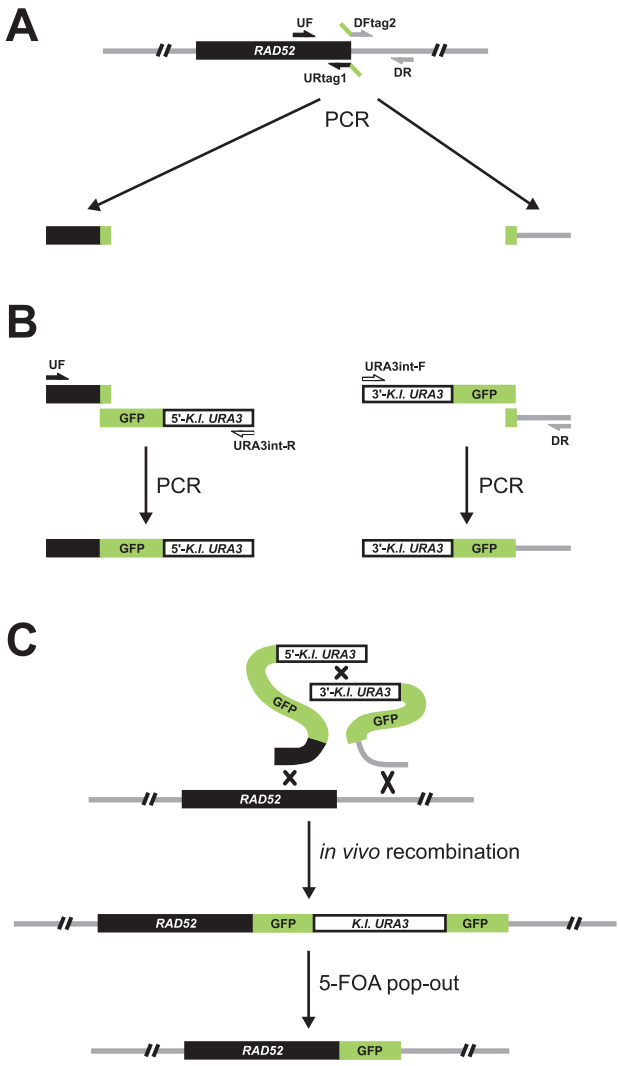

Fig. 1. GFP-tagging strategy for construction of a *RAD52-GFP* strain. (*A*) In the first PCR reactions, two pairs of PCR primers were used to amplify sequences upstream and downstream of the GFP insertion site at the 3′ end of *RAD52* (see *Materials and Methods*). (*B*) Adaptamer-mediated fusion of PCR products. The resulting upstream and downstream fragments each contained an additional 19 base pairs complementary to GFP sequence to allow the fusion of these two PCR products to DNA sequences consisting of GFP fused to either the 5′- or 3′-two-thirds of the *K. lactis URA3* gene. (*C*) Integration by *in vivo* recombination. The two DNA fragments produced in the second set of PCR reactions were transformed into *S. cerevisiae* to integrate a direct repeat of GFP immediately upstream of the endogenous *RAD52* stop codon. Subsequently, pop-out recombinants were selected on 5-FOA to remove the *URA3* marker and the extra copy of GFP.

$OD_{600} \approx 0.2$, *HO* was induced by addition of galactose to a final concentration of 2% and incubation continued for 1 h before processing of cells for microscopy. The efficiency of mating-type switching was calculated as $1 - N\mathbf{a}_{after}/(N\mathbf{a}_{after} + N\alpha_{after} - (N\alpha_{before} \cdot (N\mathbf{a}_{after} + N\alpha_{after})/(N\mathbf{a}_{before} + N\alpha_{before})))$, where N is the number of cells with the indicated mating-type before and after 1.5 h of *HO* induction, respectively.

Determination of Mitotic Recombination Rates, Sporulation Efficiency, and Meiotic Recombination Frequencies. Mitotic recombination rates were determined as described (35), except that the cells were grown at 23°C. For each strain, nine independent trials were performed. Strains analyzed for meiotic events were also grown at 23°C. Three to five trials were performed for each strain. Cells were grown in YPD overnight, diluted 100-fold into yeast extract-peptone-acetate (YEPA), and incubated until the cell density reached 2×10^7 cells/ml. The cells were washed, transferred into 2 ml SPO medium, and incubated for 2 days. At this point, the cultures were sonicated by using a Sonicator W-385 (Heat Systems/Ultrasonics) and appropriate dilutions plated on SC and SC-Leu plates to measure the meiotic recombination frequencies. Simultaneously, the fraction of sporulated cells was determined by counting the number of four-spored tetrads in each sample. Spore viability was measured by dissection of 88 tetrads for each strain. The segregation pattern of three marker pairs (*MAT***a**/*MAT*α, *LYS2*/*lys2*Δ, and *TRP1*/*trp1-1*) was determined for each tetrad, and only tetrads where all marker pairs segregated 2:2 were included in the analysis.

Results

Rad52-GFP Fusion Protein Is Biologically Functional. In the yeast *S. cerevisiae*, repair of DNA DSBs and homologous recombination depend on Rad52 function (1, 8, 9). Recently, biochemical analyses have provided clues to the function of this important protein. Thus, Rad52 binds single- and double-stranded DNA with a preference for DNA ends and stimulates DNA annealing and Rad51-catalyzed strand invasion reactions (16–18, 23, 36, 37). At present, however, only little is known about the actual role of Rad52 in recombination and repair *in vivo*. For this reason, we fused GFP to Rad52 to obtain a visual assay that allows the localization of this protein to be monitored *in vivo*.

Although the expression of *RAD52* in mitosis is constitutive, it is induced 5-fold during meiosis (38) and may be responsive to other yet unidentified modes of regulation. To ensure an expression pattern of the fusion protein similar to that of wild-type Rad52, GFP was integrated and expressed as an extension of the 3′ end of the endogenous *RAD52* gene. This was achieved by a PCR-based gene targeting technique that allows integration of GFP at any site in the genome without cloning. The method is based on the principle developed by Erdeniz and colleagues and takes advantage of the fact that PCR fragments can be fused if they have adaptamers at their ends (see Fig. 1*B*; ref. 30). Western blot analysis confirmed that the level of Rad52-GFP is equal to that of Rad52 in wild-type mitotic cells (Fig. 2*A*). Importantly, Rad52-GFP is biologically functional as it successfully replaces the wild-type protein for γ-ray-induced DNA damage repair, mating-type switching, both mitotic and meiotic recombination, and sporulation (Fig. 2*B* and Table 2).

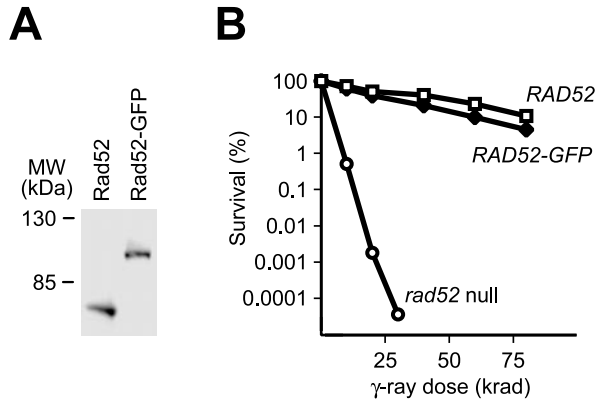

Fig. 2. Characterization of the *RAD52-GFP* strain. (*A*) Western blot analysis of Rad52 and Rad52-GFP. Protein extracts obtained from *RAD52* (W2297-12D) and *RAD52-GFP* (W2297-4A) strains were fractionated by SDS/PAGE. Rad52 and Rad52-GFP were visualized by using anti-Rad52 antibody. (*B*) γ-Ray survival curves for *RAD52* (W2297-12D), *RAD52-GFP* (W2297-4A), and *rad52* null (W2366-6B) strains. Each data point represents the mean of three independent trials.

Table 2. Characterization of *RAD52-GFP* strain

Strain properties	*RAD52*	*RAD52-GFP*	*rad52Δ*
Mitotic recombination rate,* $\times 10^{-7}$	12 ± 2	7.2 ± 1	0.017 ± 0.009
Sporulation efficiency,* %	63 ± 6	60 ± 3	0.22 ± 0.12
Germination efficiency,* %	97 ± 4	96 ± 2	nd
Meiotic recombination rate,* $\times 10^{-3}$	30 ± 4	25 ± 3	0.0004 ± 0.0003
Mating-type switching,† %	98 ± 1	99 ± 1	<0.05

nd, not determined.

*Mitotic recombination rates, sporulation and germination efficiencies, and meiotic recombination frequencies were determined for strains W2681, W2682, and W2796.

†Mating-type switching efficiencies were determined for strains W2297-12D, W2297-4A, and W2366-6B.

Rad52-GFP Forms Nuclear DNA Repair Foci During S Phase. Rad52-GFP was visualized in unsynchronized mitotic haploid cells by epifluorescence microscopy. Based on cellular morphology, cells were grouped into G_1 phase (unbudded), S (small-budded), and G_2/M (large-budded) (39). Simultaneous staining of the DNA with DAPI shows that in most cells Rad52-GFP displays a diffuse nuclear localization throughout the mitotic cell cycle (Fig. 3*A*). Interestingly, Rad52-GFP relocalizes and forms foci in 22% of S phase cells suggesting a specific role of Rad52 during DNA replication (Fig. 3*A* and Table 3). We previously provided (40) a strong link between replication and recombination by showing that Holliday junction intermediates are formed in rDNA specifically during S phase. The amount of these structures dramatically increases in a temperature-sensitive *pol12-100* strain that encodes a mutated subunit of the polymerase α complex. Because formation of these recombination intermediates depends on *RAD52* (40), we examined whether the high level of Holliday junction formation in *pol12-100* strains affects Rad52-GFP distribution. Indeed, even at the permissive temperature we found a striking increase in the frequency of Rad52-GFP foci in S phase (Table 3). Furthermore, transfer to the nonpermissive temperature results in accumulation of cells in G_2/M that contain Rad52-GFP foci. Thus, replication defects caused by an impaired polymerase α complex trigger Rad52-GFP focus formation.

To investigate the possibility that Rad52-GFP foci represent sites of DNA damage repair, we determined their formation during *RAD52*-dependent DNA repair and recombination processes. First, DNA damage was induced in the *RAD52-GFP* strains by exposing them to 20 krad of γ-irradiation. A dramatic increase in the proportion of cells containing Rad52 foci was observed, suggesting that formation of these aggregates correlates with recombinational repair (Fig. 3*B*). Surprisingly, cells on average contain only one Rad52-GFP focus despite the fact that a dose of 20 krad generates ≈10 DNA lesions per cell that require Rad52-dependent repair in order for the cell to survive (see *Materials and Methods*). This observation suggests that one focus may represent the repair of multiple lesions. To investigate this possibility, the γ-ray dose dependence of focus formation was analyzed in a dose range (2.5–160 krad) expected to generate 1.25–80 lesions per cell. If each focus represents repair of a single DNA lesion, then the number of foci is expected to increase proportionally to the γ-ray dose. First, we noticed that the process of focus formation is more easily triggered in S phase and G_2/M (Fig. 3*C*). Thus, after a dose that produces 1.25 lesions per cell (2.5 krad), more than 50% of the cells that are either in S phase or in G_2/M form at least one Rad52-GFP focus. In contrast, cells in G_1 require a 16-fold higher dose (40 krad) to reach this level. Among the cells in S or G_2/M phase that contain at least one focus, we found that a 64-fold increase in the γ-ray dose (160 krad or 80 lesions per cell) results in only a 2-fold increase in the average number of Rad52-GFP foci per cell (Fig. 3*D*). Furthermore, cells in G_1 rarely display more than one focus irrespective of γ-ray dose. Thus, the number of Rad52-GFP foci and γ-ray dose are not directly proportional, indicating that each focus likely represents the repair of multiple DNA lesions.

The biased distribution of Rad52-GFP foci in the cell cycle may reflect that haploid cells in G_1 lack a homologous chromosome that can be used as a template for recombinational repair. To evaluate this possibility, induction of Rad52 foci by γ-irradiation was studied in diploid *RAD52-GFP/RAD52-GFP* cells, where the homologous chromosome can provide a DNA substrate for recombinational repair throughout the entire cell cycle. Accordingly, the number of Rad52 foci formed in diploid cells after exposure to doses of γ-irradiation ranging from 1.25 to

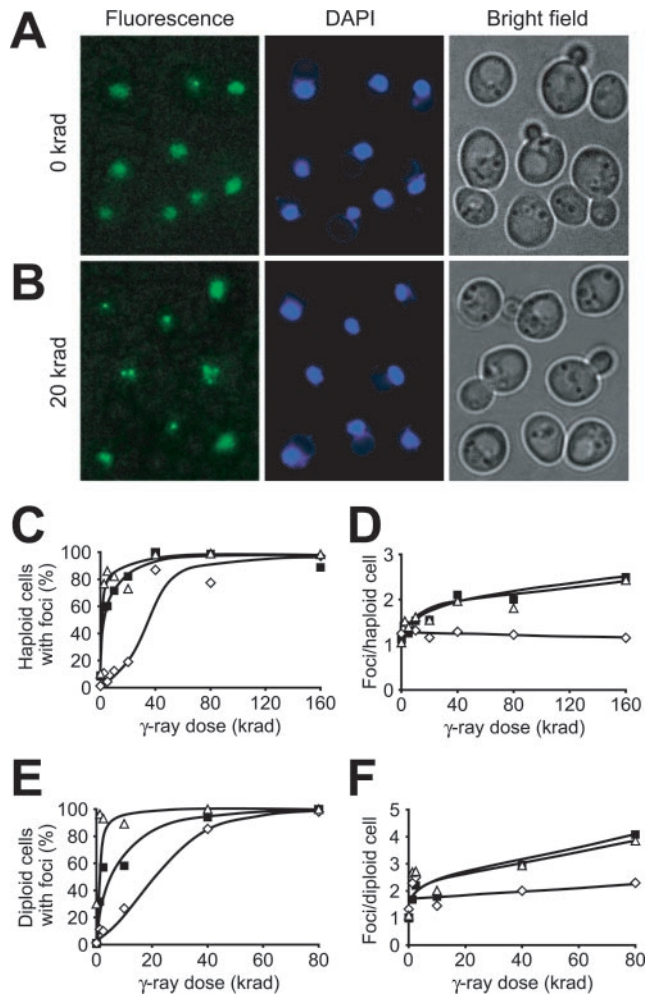

Fig. 3. Induction of nuclear Rad52-GFP foci by γ-irradiation. (*A* and *B*) Microscopy of cells (J861) expressing the Rad52-GFP fusion protein. Pictures shown are pseudocolored monochrome images: Rad52-GFP in green and DAPI-stained DNA in blue. (*A*) Diffuse nuclear localization of Rad52-GFP in nonirradiated cells. Note that one cell contains a spontaneous Rad52-GFP focus. (*B*) Relocalization of Rad52-GFP to distinct foci in cells after exposure to 20 krad of γ-irradiation. At this dose, most cells contain Rad52-GFP foci. (*C–F*) Dose dependence of Rad52 focus formation in G_1 (open diamonds), S (open triangles), and G_2/M (solid squares) phase haploid (W2297–4A) and diploid (W2682) cells. All focal planes were inspected for Rad52 foci. The number of foci observed after γ-irradiation was constant in the time frame from 15 to 90 min after irradiation and all numbers were obtained within this time frame. (*C*) Percentage of haploid cells with ≥1 focus. (*D*) The average number of Rad52 foci that are observed in haploid cells with ≥1 focus. (*E*) Percentage of diploid cells with ≥1 focus. (*F*) The average number of Rad52 foci that are observed in diploid cells with ≥1 focus.

COLLOQUIUM

Table 3. Frequencies of Rad52-GFP focus formation in G_1, S, and G_2/M cells

Strain	G_1 (unbudded)	S (small budded)	G_2/M (large budded)
Wild type,* 23°C	0/316 (0%)	24/109 (22%)	1/82 (1%)
pol12-100,† 23°C	0/100 (0%)	21/43 (49%)	5/50 (13%)
pol12-100,† 37°C	2/67 (3%)	5/43 (12%)	97/157 (62%)
Wild type,* 37°C	0/284 (0%)	10/87 (11%)	11/67 (16%)
mec1 sml1,‡ 23°C	15/186 (8%)	29/56 (52%)	19/34 (54%)
sml1,§ 23°C	2/202 (1%)	19/77 (25%)	4/81 (5%)

*Strain W2297-4A.
†Strain UM10-25D.
‡Strain W2381-10B. The essential function of *MEC1* is suppressed by mutation of *sml1*, an inhibitor of ribonucleotide reductase, but importantly, *mec1 sml1* strains still fail to arrest at the G_1 and G_2/M checkpoints during genotoxic stress (68). Hence, we employed the *mec1 sml1* strain background to test the effect of a DNA damage checkpoint defect on Rad52-GFP focus formation.
§Strain W2382-2A.

80 krad (equivalent to 1.25–80 lesions per cell) was determined. Interestingly, the number of Rad52 foci induced by γ-irradiation in diploid cells is approximately twice the number observed in haploid cells, but is still not proportional to the number of DNA lesions induced (compare Figs. 3*D* and 2*F*). However, like haploid G_1 cells, diploid G_1 cells require a 16-fold higher dose than S phase cells to reach the level where 50% of the cells contain at least one focus (Fig. 3*E*). This observation demonstrates that DNA DSBs induced in the presence of a homologous DNA substrate alone is not sufficient to elicit Rad52 focus formation. Indeed, the cell also needs to be in the proper phase of the cell cycle to form this structure.

Numerous Rad52 Foci Are Formed During Meiotic Recombination. Because γ-irradiation produces a variety of lesions (41) that are likely to have different repair requirements, we tested Rad52-GFP focus formation specifically during DNA DSB repair. Multiple DSBs are generated by Spo11 during the onset of meiotic recombination at early prophase of meiosis I (42, 43). Efficient repair of these breaks requires Rad52 (44). After shifting *RAD52-GFP/RAD52-GFP* diploid strains to SPO medium, we found that Rad52-GFP relocalizes to form ≈15 foci per nucleus (Fig. 4*A*). The number of meiotic Rad52-GFP foci observed *in vivo* is similar to that seen after immunostaining of Rad52 in nuclear spreads (45). We next examined meiotically induced *spo11/spo11* mutants, which are blocked for DSB formation (46). In contrast to *SPO11/SPO11* diploids, multiple Rad52-GFP foci were not observed and the occasional single focus observed in these mutants is likely due to repair of DNA damage that arose during premeiotic S phase (data not shown).

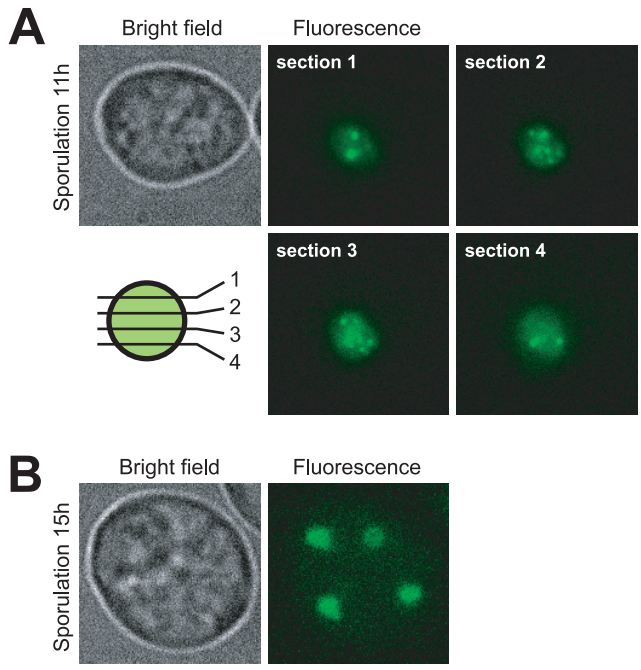

Fig. 4. Formation of Rad52-GFP foci during sporulation. Microscopy of sporulating cells (W2682) expressing the Rad52-GFP fusion. (*A*) A representative sporulating cell before the first meiotic division after 11 h in SPO medium. Four optical sections separated by 0.4 μm are displayed (see schematic). (*B*) A four-spored tetrad after 15 h in SPO medium is displayed showing that Rad52 foci have disassembled after the second meiotic division.

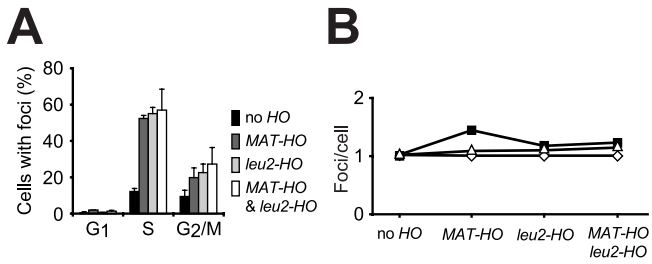

Fig. 5. Rad52-GFP foci induced by the *HO* endonuclease. (*A*) The percentages of cells in G_1, S, and G_2/M containing foci after induction of *HO* in strains with no (W2334–1D), one (W2322–5B and W2613–22A), or two (W2322–8A) *HO*-cut sites, are shown. (*B*) The average number of Rad52 foci that are observed in G_1 (open diamonds), S (open triangles), and G_2/M (solid squares) phase cells with ≥1 focus.

Rad52 Foci Form After Induction of Specific DSBs by the *HO* Endonuclease. Well defined DSBs were also induced by the *HO* endonuclease (47) in a *RAD52-GFP* strain. Two different *HO*-cut sites were investigated. One is the *HO*-cut site that exists naturally at the mating-type locus (*MAT-HO*). When this site is cleaved by the *HO* endonuclease, the resulting DSB is repaired by gene conversion (48). The other *HO*-cut site is situated in a *LEU2* direct repeat at the *LEU2* locus (*leu2-HO*). In this case, the *HO* endonuclease induces a DSB that is repaired by single-strand annealing (35). Strains were constructed that contain no accessible *HO*-cut sites, a single *HO*-cut site (either *MAT-HO* or *leu2-HO*), or two *HO*-cut sites (both *MAT-HO* and *leu2-HO*). After induction of the *HO* endonuclease in strains that contained one *HO*-cut site at either *MAT* or *leu2*, Rad52 foci were observed in 50–60% of S phase cells and 20–30% of G_2/M phase cells (Fig. 5*A*). In contrast, foci are formed in only 15% of S and 10% of G_2/M cells in the strain that contains no accessible *HO*-cut site. Similar to what was observed after γ-irradiation (Fig. 3*C*), very few G_1 cells form foci upon *HO* induction. Thus, *HO*-induced breaks, like γ-ray-induced DNA damage, preferentially generate Rad52 foci in S phase. Interestingly, when the strains containing two *HO*-cut sites were analyzed, the average number of foci observed per cell did not double when compared with strains that contain only one *HO*-cut site (Fig. 5*B*). Hence, the number of Rad52-GFP foci formed *in vivo* is largely independent of the number of DNA DSBs, regardless of whether they are induced by γ-irradiation or by *HO*. This result suggests that one focus may represent the repair of multiple DNA lesions within a limited number of centers in the nucleus.

Absence of the *MEC1* DNA Damage Checkpoint Gene Results in Increased Rad52 Focus Formation. It is well known that DNA lesions such as single-strand nicks, abasic sites, and photolesions trigger cell-cycle checkpoints (49). Because a synthetic lethal interaction between a *rad52* mutation and mutations of *MEC1*, a central DNA damage checkpoint gene (50), has been observed

(51), we monitored the formation of Rad52-GFP foci in a *mec1* mutant strain. The frequency of Rad52-GFP foci increases from 22% and 1% in wild-type S and G_2/M phase cells, respectively, to 52% and 54% in the corresponding *mec1* cells (Table 3). This observation shows that Rad52 focus formation does not depend on Mec1. In addition, the ability of Rad52-GFP to form foci after γ-irradiation is also intact in *mec1* mutant cells (data not shown). Finally, the observation of an increase in spontaneous focus formation in the absence of Mec1 suggests that more lesions requiring Rad52-dependent repair are generated throughout the S and G_2 phases in *mec1* mutant strains.

Discussion

We have tagged *RAD52* with GFP by using a PCR-based cloning-free gene targeting method and showed that the resulting Rad52-GFP is biologically functional and localizes exclusively to the nucleus. In most cells, Rad52-GFP is evenly distributed throughout the nucleus, but occasionally it relocalizes spontaneously and forms bright foci. In this study, we demonstrate that DNA DSBs induced by γ-irradiation, by the *HO* endonuclease, or by Spo11 during meiosis all result in a dramatic stimulation of Rad52-GFP focus formation. Moreover, DNA damage produced by defective DNA replication in *pol12-100* strains also results in an increased frequency of Rad52-GFP focus formation. Notably, the *pol12-100* mutation causes accumulation of Holliday junction intermediates as part of a Rad52-dependent recombinational repair process (40). These experiments provide compelling evidence that Rad52-GFP foci represent sites of active DNA repair *in vivo*. In addition, we show that repair of *HO* endonuclease-induced breaks that proceeds via different pathways (gene conversion and single-strand annealing) causes Rad52-GFP focus formation. It is therefore likely that Rad52 aggregation is a common denominator of Rad52 activity during DNA repair and recombination. The importance of this feature is highlighted by its conservation from yeast to mammals (52, 53), where DNA damage also induces formation of GFP-Rad52 foci. The functionality of GFP-Rad52 foci in mammalian cells is strengthened by immunostaining experiments that showed partial colocalization of mammalian GFP-Rad52 foci with Rad51 and Rad50 foci. This result supports the notion of a central role of Rad52 in recombinational DNA repair in higher eukaryotes, despite the weak phenotype observed in its absence. Interestingly, mammalian Rad52 is excluded from nucleoli during late G_1, but distributes evenly in the nucleus during S phase and in G_0. In contrast, yeast Rad52 seems to colocalize evenly with the DNA throughout the entire mitotic cell cycle. This difference suggests a more specialized role of *RAD52* in mammalian cells where different homologues or isoforms of the gene could have distinct functions (54).

Quantitative analysis of Rad52 foci formed after induction of DSBs by the *HO* endonuclease and by γ-irradiation demonstrates that a single DNA lesion can be visualized by using Rad52-GFP as a molecular marker. It has been shown (17, 18) that Rad52 heptamers bind preferentially to DNA ends. However, it is unlikely that a single Rad52-GFP heptamer emits sufficient light to be visualized and we therefore propose that accumulation of several Rad52 heptamers at a DNA lesion is required to efficiently complete the repair process *in vivo*. This view is supported by the fact that Rad52 also aggregates on DNA in *vitro* (26, 55, 56). Perhaps binding of a Rad52 heptamer to a DNA end may represent an early stage in the construction of a larger Rad52 complex and that DNA ends simply act as a nucleation site for Rad52.

The aggregation of Rad52 at a single lesion is intriguing. It was shown (16) that Rad52 stimulates DNA annealing. This activity may contribute to recombination in several different ways. Firstly, annealing may facilitate the search for homology. Secondly, after the invasion by one 3′ tail during DNA DSB repair, annealing is required for the resulting D-loop to establish contact with the other 3′ single-stranded tail. Thirdly, annealing is important in the major pathway for direct repeat recombination: single-strand annealing. Because the rate of annealing depends on the number of bases actively available for this process, the collaboration of a large number of Rad52 heptamers in annealing could expose more bases to allow single-stranded regions to pair.

Furthermore, we were surprised to find that only a limited number of Rad52 foci develop even after the introduction of multiple lesions. Most strikingly, a γ-ray dose expected to create 80 lesions only induces formation of two foci per cell, on average (Fig. 3*D*). The discrepancy between the number of induced lesions and the number of observed Rad52 foci could indicate that the optical sensitivity of the assay only allows detection of a limited number of Rad52 catalyzed repair reactions. However, we consider this possibility unlikely as Rad52 foci are easily detected in >50% of S phase cells that contain a single DSB (Figs. 3*C* and 5*A*). Instead, we envision that each Rad52 focus represents a center of recombinational repair that is capable of processing multiple DNA lesions. Perhaps the aggregation of Rad52 heptamers (and probably other repair proteins) acts to attract other lesions for repair within one focus. A major challenge will be to understand the advantage of concentrating the recombination machinery in one or a few locations.

The fact that spontaneous Rad52-GFP foci are most frequently observed in S phase cells and only rarely in G_1 cells implies a coupling between recombinational repair and DNA replication (Fig. 3*C*). Likewise, γ-ray stimulation of Rad52-GFP focus formation in S cells requires much lower doses than in G_1 cells. Furthermore, elimination of the *MEC1* DNA damage checkpoint, which operates in all phases of the cell cycle, does not increase the number of G_1 cells that contain Rad52-GFP foci. We also showed that lesions produced during defective DNA replication in *pol12-100* strains result in a dramatic increase in the number of Rad52-GFP foci. Several other studies have provided evidence for a link between replication and recombination (see other papers in this colloquium). In particular, many of the proteins involved in homologous recombination are also involved in replication (e.g., RP-A, Polδ, Polε, Polα, Rad27, and DNA primase; refs. 20 and 57–59). Furthermore, this study and others (40, 60–63) have demonstrated that the replication process itself can produce DNA lesions that require recombinational repair. In fact, DNA repair centers in S phase cells may be directly linked to replication foci, where many adjacent origins are organized into a few replication centers (64). The coupling of recombinational DNA repair to S phase may be advantageous to the cell. For example, DNA DSB repair may be delayed until S phase, where breaks are detected automatically during the replication process and trigger checkpoints that allow them to be repaired before proceeding into G_2/M (49, 65). In addition, the coordination of these two processes is logical, because replication *per se* is likely the major source of lesions that require recombinational repair.

In meiotic cells, homologous recombination is initiated by the formation of numerous Spo11-induced DNA DSBs in early prophase. It has been estimated that approximately 200 recombination events occur per meiotic cell (66). We have shown that, in meiosis, numerous Rad52-GFP foci are formed. Development of these foci depends on the presence of Spo11. However, the number (≈15) of foci observed (Fig. 4*A*) does not reflect the number of recombination events, suggesting that recombinational repair centers also exist in meiotic cells. It is tempting to speculate that one recombination center is formed for each pair of homologous chromosomes. Such a scheme might enhance synapsis formation and at the same time lower the frequency of interchromosomal ectopic recombination.

The experimental strategy presented in this paper provides a powerful tool for elucidating the coordination of DNA repair, recombination, and replication *in vivo*. In the future, it shall be interesting to investigate how proteins that are involved in these important processes localize, both temporally and spatially, with respect to Rad52 foci.

We thank members of the Rothstein laboratory and Aleksei Aleksenko for helpful discussions concerning this work, as well as Liza Pon and members of her laboratory for skillful assistance during microscopy. We also thank Roger Tsien for providing the enhanced GFP clone. This research was supported by grants from the Dagmar Marshall Foundation, the Leo Research Foundation, the Neye Foundation, the Danish Cancer Society, and the Alfred Benzon Foundation (to M.L.); grants from the Tonnessen Foundation, the Danish Medical Research Council and the Danish Technical Research Council (to U.H.M.); Grants HG01620 and GM50237 from the National Institutes of Health (to R.R.); and National Institutes of Health Shared Instrument Grant S10 RR10506 and National Institutes of Health Grant P30 CA13696 to the Columbia Cancer Center.

1. Petes, T. D., Malone, R. E. & Symington, L. S. (1991) in *The Molecular & Cellular Biology of the Yeast Saccharomyces: Genome Dynamics, Protein Synthesis and Energetics*, eds. Broach, J. R., Pringle, J. R. & Jones, E. W. (Cold Spring Harbor Lab. Press, Plainview, NY), Vol. 1, pp. 407–521.
2. Gangloff, S., Zou, H. & Rothstein, R. (1996) *EMBO J.* **15,** 1715–1725.
3. Le, S., Moore, J. K., Haber, J. E. & Greider, C. W. (1999) *Genetics* **152,** 143–152.
4. Szostak, J. W., Orr-Weaver, T. L., Rothstein, R. J. & Stahl, F. W. (1983) *Cell* **33,** 25–35.
5. Resnick, M. A. & Martin, P. (1976) *Mol. Gen. Genet.* **143,** 119–129.
6. Game, J. C. (1993) *Semin. Cancer Biol.* **4,** 73–83.
7. Bai, Y. & Symington, L. S. (1996) *Genes Dev.* **10,** 2025–2037.
8. Sung, P., Trujillo, K. M. & Van Komen, S. (2000) *Mutat. Res.* **451,** 257–275.
9. Paques, F. & Haber, J. E. (1999) *Microbiol. Mol. Biol. Rev.* **63,** 349–404.
10. Milne, G. T. & Weaver, D. T. (1993) *Genes Dev.* **7,** 1755–1765.
11. Shen, Z., Cloud, K. G., Chen, D. J. & Park, M. S. (1996) *J. Biol. Chem.* **271,** 148–152.
12. Yamaguchi-Iwai, Y., Sonoda, E., Buerstedde, J. M., Bezzubova, O., Morrison, C., Takata, M., Shinohara, A. & Takeda, S. (1998) *Mol. Cell. Biol.* **18,** 6430–6435.
13. Rijkers, T., Van Den Ouweland, J., Morolli, B., Rolink, A. G., Baarends, W. M., Van Sloun, P. P., Lohman, P. H. & Pastink, A. (1998) *Mol. Cell. Biol.* **18,** 6423–6429.
14. van den Bosch, M., Vreeken, K., Zonneveld, J. B., Brandsma, J. A., Lombaerts, M., Murray, J. M., Lohman, P. H. & Pastink, A. (2001) *Mutat. Res.* **461,** 311–323.
15. Suto, K., Nagata, A., Murakami, H. & Okayama, H. (1999) *Mol. Biol. Cell* **10,** 3331–3343.
16. Mortensen, U. H., Bendixen, C., Sunjevaric, I. & Rothstein, R. (1996) *Proc. Natl. Acad. Sci. USA* **93,** 10729–10734.
17. Van Dyck, E., Stasiak, A. Z., Stasiak, A. & West, S. C. (1999) *Nature (London)* **398,** 728–731.
18. Parsons, C. A., Baumann, P., Van Dyck, E. & West, S. C. (2000) *EMBO J.* **19,** 4175–4181.
19. Shinohara, A., Ogawa, H. & Ogawa, T. (1992) *Cell* **69,** 457–470.
20. Firmenich, A. A., Elias-Arnanz, M. & Berg, P. (1995) *Mol. Cell. Biol.* **15,** 1620–1631.
21. Hays, S. L., Firmenich, A. A., Massey, P., Banerjee, R. & Berg, P. (1998) *Mol. Cell. Biol.* **18,** 4400–4406.
22. Sung, P. (1997) *J. Biol. Chem.* **272,** 28194–28197.
23. New, J. H., Sugiyama, T., Zaitseva, E. & Kowalczykowski, S. C. (1998) *Nature (London)* **391,** 407–410.
24. Song, B. & Sung, P. (2000) *J. Biol. Chem.* **275,** 15895–15904.
25. Stasiak, A. Z., Larquet, E., Stasiak, A., Muller, S., Engel, A., Van Dyck, E., West, S. C. & Egelman, E. H. (2000) *Curr. Biol.* **10,** 337–340.
26. Shinohara, A., Shinohara, M., Ohta, T., Matsuda, S. & Ogawa, T. (1998) *Genes Cells* **3,** 145–156.
27. Sherman, F., Fink, G. R. & Hicks, J. B. (1986) *Methods in Yeast Genetics* (Cold Spring Harbor Lab. Press, Plainview, NY).
28. Ormo, M., Cubitt, A. B., Kallio, K., Gross, L. A., Tsien, R. Y. & Remington, S. J. (1996) *Science* **273,** 1392–1395.
29. Hudson, J. R., Jr., Dawson, E. P., Rushing, K. L., Jackson, C. H., Lockshon, D., Conover, D., Lanciault, C., Harris, J. R., Simmons, S. J., Rothstein, R. & Fields, S. (1997) *Genome Res.* **7,** 1169–1173.
30. Erdeniz, N., Mortensen, U. H. & Rothstein, R. (1997) *Genome Res.* **7,** 1174–1183.
31. Christianson, T. W., Sikorski, R. S., Dante, M., Shero, J. H. & Hieter, P. (1992) *Gene* **110,** 119–122.
32. Lim, C. R., Kimata, Y., Oka, M., Nomaguchi, K. & Kohno, K. (1995) *J. Biochem. (Tokyo)* **118,** 13–17.
33. Weiffenbach, B. & Haber, J. E. (1981) *Mol. Cell. Biol.* **1,** 522–534.
34. Jensen, R. E. & Herskowitz, I. (1984) *Cold Spring Harbor Symp. Quant. Biol.* **49,** 97–104.
35. Smith, J. & Rothstein, R. (1999) *Genetics* **151,** 447–458.
36. Sugiyama, T., New, J. H. & Kowalczykowski, S. C. (1998) *Proc. Natl. Acad. Sci. USA* **95,** 6049–6054.
37. Shinohara, A. & Ogawa, T. (1998) *Nature (London)* **391,** 404–407.
38. Cole, G. M., Schild, D. & Mortimer, R. K. (1989) *Mol. Cell. Biol.* **9,** 3101–3104.
39. Lew, D. J., Weinert, T. & Pringle, J. R. (1997) in *The Molecular and Cellular Biology of the Yeast Saccharomyces*, eds. Pringle, J. R., Broach, J. R. & Jones, E. W. (Cold Spring Harbor Lab. Press, Plainview, NY), Vol. 3, pp. 612.
40. Zou, H. & Rothstein, R. (1997) *Cell* **90,** 87–96.
41. Ward, J. F. (1995) *Radiat. Res.* **142,** 362–368.
42. Keeney, S., Giroux, C. N. & Kleckner, N. (1997) *Cell* **88,** 375–384.
43. Smith, K. N. & Nicolas, A. (1998) *Curr. Opin. Genet. Dev.* **8,** 200–211.
44. Borts, R. H., Lichten, M. & Haber, J. E. (1986) *Genetics* **113,** 551–567.
45. Gasior, S. L., Wong, A. K., Kora, Y., Shinohara, A. & Bishop, D. K. (1998) *Genes Dev.* **12,** 2208–2221.
46. Cao, L., Alani, E. & Kleckner, N. (1990) *Cell* **61,** 1089–1101.
47. Kostriken, R., Strathern, J. N., Klar, A. J., Hicks, J. B. & Heffron, F. (1983) *Cell* **35,** 167–174.
48. Haber, J. E. (1992) *Trends Genet.* **8,** 446–452.
49. Paulovich, A. G., Toczyski, D. P. & Hartwell, L. H. (1997) *Cell* **88,** 315–321.
50. Weinert, T. (1998) *Cell* **94,** 555–558.
51. Merrill, B. J. & Holm, C. (1999) *Genetics* **153,** 595–605.
52. Liu, Y., Li, M., Lee, E. Y. & Maizels, N. (1999) *Curr. Biol.* **9,** 975–978.
53. Liu, Y. & Maizels, N. (2000) *EMBO Rep.* **11,** 85–90.
54. Kito, K., Wada, H., Yeh, E. T. & Kamitani, T. (1999) *Biochim. Biophys. Acta* **1489,** 303–314.
55. Kim, W. J., Lee, S., Park, M. S., Jang, Y. K., Kim, J. B. & Park, S. D. (2000) *J. Biol. Chem.* **275,** 35607–35611.
56. Van Dyck, E., Hajibagheri, N. M., Stasiak, A. & West, S. C. (1998) *J. Mol. Biol.* **284,** 1027–1038.
57. Smith, J. & Rothstein, R. (1995) *Mol. Cell. Biol.* **15,** 1632–1641.
58. Wold, M. S. (1997) *Annu. Rev. Biochem.* **66,** 61–92.
59. Holmes, A. M. & Haber, J. E. (1999) *Cell* **96,** 415–424.
60. Chen, C., Umezu, K. & Kolodner, R. D. (1998) *Mol. Cell* **2,** 9–22.
61. Chen, C., Merrill, B. J., Lau, P. J., Holm, C. & Kolodner, R. D. (1999) *Mol. Cell. Biol.* **19,** 7801–7815.
62. Symington, L. S. (1998) *Nucleic Acids Res.* **26,** 5589–5595.
63. Tishkoff, D. X., Filosi, N., Gaida, G. M. & Kolodner, R. D. (1997) *Cell* **88,** 253–263.
64. Newport, J. & Yan, H. (1996) *Curr. Opin. Cell Biol.* **8,** 365–368.
65. Raghuraman, M. K., Brewer, B. J. & Fangman, W. L. (1994) *Genes Dev.* **8,** 554–562.
66. Roeder, G. S. (1997) *Genes Dev.* **11,** 2600–2621.
67. Thomas, B. J. & Rothstein, R. (1989) *Cell* **56,** 619–630.
68. Zhao, X., Muller, E. G. & Rothstein, R. (1998) *Mol. Cell* **2,** 329–340.